Thermochimica Acta 557 (2013) 61–67

Contents lists available at SciVerse ScienceDirect

Thermochimica Acta

journal homepage: www.elsevier.com/locate/tca

Kinetic study on the chlorination of β-spodumene for lithium extraction with Cl_2 gas

L.I. Barbosa[a,b,*], N.G. Valente[b], J.A. González[a,b]

[a] Instituto de Investigaciones en Tecnología Química (INTEQUI-CONICET), Universidad Nacional de San Luis, Chacabuco y Pedernera, 5700 San Luis, Argentina
[b] Instituto de Ciencias Básicas, Universidad Nacional de Cuyo, Padre Jorge Contreras 1300, Parque General San Martín, M5502JMA Mendoza, Argentina

ARTICLE INFO

Article history:
Received 9 October 2012
Received in revised form 5 January 2013
Accepted 31 January 2013
Available online 15 February 2013

Keywords:
Kinetics
Extraction
Lithium
β-Spodumene

ABSTRACT

In this paper, the kinetics chlorination of β-spodumene for the extraction of lithium has been studied using gaseous chlorine as chlorinating agent. The effect of chlorine flow rate, temperature, mass of the sample, and partial pressure of Cl_2 was investigated. The study of the effect of chlorine flow rate indicated that the chlorination of β-spodumene may be carried out in the presence of active chlorinating species The chlorine partial pressure was found to have an appreciable effect on the system reactivity. The temperature was found to be the most important variable affecting the reaction rate. The β-spodumene chlorination process by Cl_2 was characterized by an apparent activation energy of about 359 kJ/mol in the range from 1000 to 1100 °C. Reaction was of non-catalytic gas–solid nature and experimental data fitted the sequential nucleation and growth model.

1. Introduction

Lithium possesses properties that make it highly required for commercial applications. Lithium and its compounds are mainly used in ceramic (frits) and glass manufacturing; to lower the melting point of the production of synthetic rubber, plastics and pharmaceutical products; in the synthesis of many organic compounds; in lubricants and greases used for working in extreme temperature and change conditions; in the production of both primary and secondary batteries; and in air conditioning and dehumidification systems. Principally, the key to the market expansion has been the increase in the use of lithium in rechargeable batteries and the demand growth from China [1].

Lithium is a comparatively rare element, although it is found in many rocks and some brines, but always in very low concentrations. The most abundant of the lithium minerals is spodumene ($LiAlSi_2O_6$), a lithium pyroxene containing up to 3.73% Li (8.03% Li_2O). However, the worldwide commercial extraction of lithium is carried out through brines at present, because of lower production costs as compared with mining and processing costs for lithium ores. As lithium market is growing increasingly, lithium bearing minerals might be once again an alternative raw material for its production.

Extraction of metals from metals oxides resided in ores or minerals by chlorination has proved to be effective principally because of the high reactivity and strong affinity of chlorine towards metals oxides and silicates and because the production of water soluble chlorides [2–5]. The chlorination of lithium bearing ores has been used through various chlorinating methods to selectively extract lithium as lithium chloride at elevated temperatures [6–9]. Taking in consideration this background information then, it is necessary to understand thoroughly the chlorination reaction implied in a given process of lithium recovery from lithium ores for reactor design and to set the operation variables.

Our work was focused on the kinetic study of the chlorination of β-spodumene for the extraction of lithium with pure chlorine gas. Experiments were carried out in a fixed-bed reactor at high temperature domain. The quantitative data concerning the effects of Cl_2 flow rate, temperature, the mass of the sample as well as the Cl_2 partial pressure, on the reaction rate of β-spodumene with chlorine were revealed from this experimental study within the temperatures ranging from 1000 to 1100 °C.

2. Thermodynamic analysis

The thermodynamic analysis of the β-spodumene chlorination with chlorine gas was carried out between 25 and 1200 °C through the software HSC Chemistry for Windows 5.1 [10]. Following the previous work [9], we will consider the following reactions:

$$LiAlSi_2O_6(B) + 1/2Cl_2(g) = 1/4O_2(g) + LiCl + 1/6Al_6Si_2O_{13} + 5/3SiO_2(CRS) \quad (1)$$

* Corresponding author. Present address: Chacabuco y Pedernera, 5700 San Luis, Argentina. Tel.: +54 2664 426711; fax: +54 2664 426711.
E-mail address: lbarbosa@unsl.edu.ar (L.I. Barbosa).

0040-6031/$ – see front matter © 2013 Elsevier B.V. All rights reserved.
http://dx.doi.org/10.1016/j.tca.2013.01.033

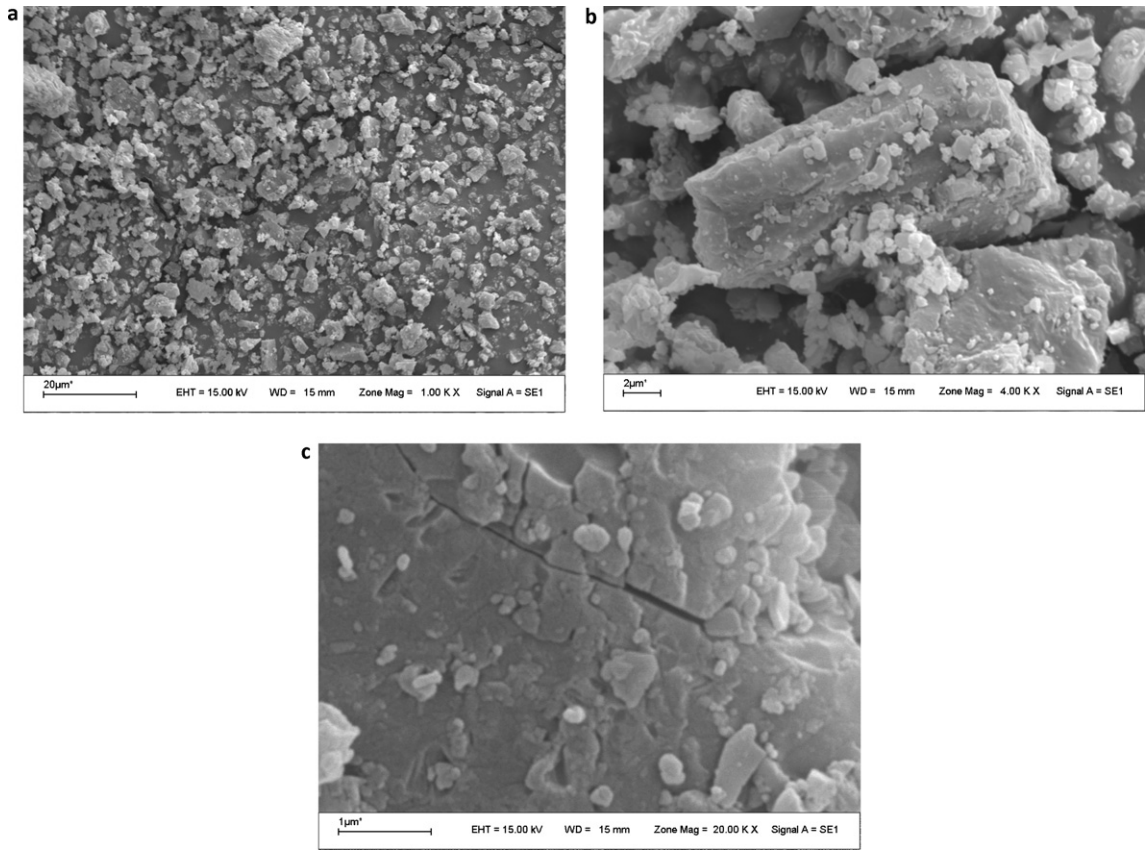

Fig. 1. Morphology of the β-spodumene particles: (a) overall view; (b) morphology of particles of different sizes; (c) superficial appearance of a particle.

$$\Delta G^{\circ} = (0.0085(T) - 4.63)(\text{kcal/mol}\ \beta - \text{spodumene})\ \text{for LiCl(s)} \quad (2)$$

$$\Delta G^{\circ} = (-0.0088(T) - 2.02)(\text{kcal/mol}\ \beta - \text{spodumene})\ \text{for LiCl(l)} \quad (3)$$

$$\Delta G^{\circ} = (-0.025(T) + 36.2)(\text{kcal/mol}\ \beta - \text{spodumene})\ \text{for LiCl(g)} \quad (4)$$

$$1/6Al_6Si_2O_{13} + 3/2\,Cl_2(g) = 1/3\,SiO_2(CRS) + 3/4O_2(g) + AlCl_3(g) \quad (5)$$

$$\Delta G^{\circ} = (-0.023(T) + 52.8)(\text{kcal/mol}) \quad (6)$$

where $LiAlSi_2O_6$(B) is β-spodumene, SiO_2(CRS) silica in its cristobalite phase, and $Al_6Si_2O_{13}$ mullite.

It can be seen from thermodynamic calculations that it is possible to obtain LiCl(l) but not LiCl(g) by chlorination of β-spodumene with Cl_2, in the studied temperature range. However, in previous experimentation, it has been detected the mass loss due to the volatilization of LiCl and O_2 [9]. This difference lays on the fact that at temperatures above 900 °C, the LiCl(l) has a sufficient vapor pressure to be entrained by the gaseous stream of chlorine together with O_2, leaving both the reaction zone, as can be seen from Eq. (7) that shows the variation of LiCl(l) vapor pressure with the temperature determined experimentally within the temperature range of this work [11].

$$\log P(\text{atm}) = (5.031 \pm 0.148) - (8387 \pm 134)/T. \quad (7)$$

The thermodynamic analysis also showed that the chlorination of mullite is not favored in the whole studied range (Eq. (6)); therefore the products of β-spodumene chlorination reaction are: LiCl (l), mullite and cristobalite in solid state, and O_2 (g).

3. Materials

The mineral used in this work was spodumene from San Luis, Argentina, containing 7.25% Li_2O and about 2% impurities, which consist mainly of Fe, Ca and Mg. This naturally occurring alpha crystalline form was calcined to produce spodumene in its beta crystalline form, which has been properly characterized in our previous work [9]. The result of the characterization of β-spodumene through SEM is presented in Fig. 1. It shows that the solid is made up of particles of different sizes that vary from 2 to 20 μm with sharp edges and stepped surface. The BET analysis showed a low specific area (3.04 m^2/g) indicating a week porosity of β-spodumene grains.

The gasses used in the different chlorination assays were chlorine 99.5% (Cofil, Argentina) and nitrogen 99, 99% (Air Liquide, Argentina).

4. Equipment

The reactor consisted of a quartz tube (o.d. 16 mm, wall thickness 1 mm, and length 440 mm) which was placed in an electric furnace equipped with a temperature controller. The β-spodumene sample was held in a quartz crucible (length 70 mm, width 10 mm, and depth 6 mm) which was located inside the reactor tube. Chlorine stored in a cylinder was introduced to the inlet of the reactor through Teflon tubing. Mass flowmeters and metering valves were used to control the flowrate. A scrubber with 5% caustic soda solution neutralized the exit gas. An analytical balance (Mettler Toledo

AB204-S/FACT) was used for the measurement of the sample mass before and after experiments. The balance has a maximum sensitivity of 0.0001 g. Reactants and products were analyzed by SEM (microscope LEO 1450VP), EPMA (EDS spectrometer Genesis 2000 and WDS, INCA wave 700), and BET (Micromeritis Gemini V Surface area and pore analyzer).

5. Procedure

The reactor was heated to the research temperature at a heating rate of 10 °C/min. Once the set temperature was reached and stabilized, the quartz crucible containing approximately 0.4 g of the sample was slowly inserted into the middle of the reactor and then kept in nitrogen atmosphere, using a N_2 flow rate of 100 ml/min for 15 min. Then, the nitrogen flow was shut off and Cl_2 was fed into the reactor at the desired flow rate. After specified reaction time, Cl_2 was replaced by nitrogen again to purge the system for 15 min. At the end of this period, the sample was taken out from the reactor, cooled down and weighted.

In our previous studies we find a linear correlation between the total mass loss due to both the chlorination of lithium and the chlorination of impurities, and the mass loss due to solely to the chlorination of lithium [9]. This correlation is based on the mass of the chlorinated sample observed at the end of the chlorination assay, and on the content of Li_2O in the chlorination residues, which in turn was determined through atomic absorption. Thus, the extent of lithium chlorination was calculated as follows:

$$X = \%\Delta m_{Li_2O} / X^0 \quad (8)$$

where X is the conversion of Li_2O; X^0 the initial concentration of Li_2O in β-spodumene; $\%\Delta m_{Li_2O}$ mass loss percentage of Li_2O. The dependence of $\%\Delta m_{Li_2O}$ with $\%\Delta m$ (mass loss percentage of β-spodumene) for each temperature is shown in the following Table 1.

6. Results and discussion

6.1. Effect of chlorine flow rate

In the experimental determination of kinetic parameters it is very important to ensure that the measurements are carried out under conditions such that the overall rate is indeed controlled by chemical kinetics, i.e. pore diffusion and gas phase mass transfer do not play an appreciable role. This could be achieved by operating the gas-solid reaction system at sufficiently high gas flow rates, so that any further increase in gas flow rate does not produce an increase in the overall reaction rate [12]. As the mass transfer phenomena are promoted at high temperature, the effect of the gas flow rate on β-spodumene chlorination was studied at 1100 °C, in the range of 25–200 ml/min. It can be noted from Fig. 2 that at low flow rates, the reaction rate increased with the flow rate because the reaction rate was controlled by chlorine availability. However, beyond a flow rate of about 100 ml/min, the reaction rate, instead of becoming constant, actually decreased. Similar results have been reported in other works [13–19]. The reason for this could be the following: a gaseous intermediate whose concentration controls

Table 1
Dependence of mass loss of Li_2O with total mass loss.

$\%\Delta m_{Li_2O} = a(\%\Delta m) + b$		
T (°C)	a	b
1000	0.8848	−1.6411
1025	0.9113	−1.6411
1050	0.9113	−1.0258
1075	0.9113	−1.0258
1100	0.7163	−0.0204

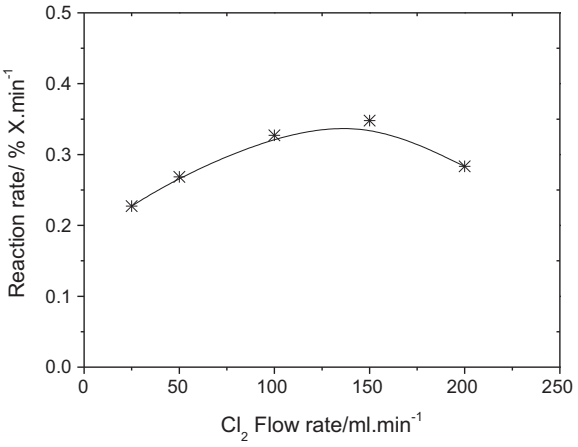

Fig. 2. Effect of Cl_2 flow rate on the reaction of β-spodumene chlorination at 1100 °C.

the rate of reaction gets diluted at the higher flow rates resulting in lower chlorination rates. Such an explanation has been proposed by Sparling and Glastonbury. Further, at high flow rates, most of the gas bypasses the charge and the residence time is also quite low. Moreover, the gaseous intermediate controlling the reaction rate may be active chlorine. The formation of active chlorine at temperatures near 1000 °C has been proposed by other authors in the direct chlorination as well as in the carbochlorination of oxides [20,21]. Accordingly, working with a flow rate of 100 ml/min is sufficient to minimize the effect of external mass transfer and appropriate to avoid that the active chlorinating species become diluted.

6.2. Effect of temperature

The influence of temperature on the chlorination of β-spodumene was investigated in the range from 1000 to 1100 °C. The other chlorination process conditions were as follows: flow rate, 100 ml/min; chlorine molar fraction, 1; and mass of the sample, 0.4 g. The results have been expressed as conversion of Li_2O vs. time, and are shown in Fig. 3. In this figure, it can be observed that a noticeable increase on the reaction rate is produced with the increase of temperature.

6.3. Effect of the mass of the sample

Fig. 4 shows the effect of the mass of the sample on the system reactivity at 1100 °C, working with a flow rate of 100 ml/min. It

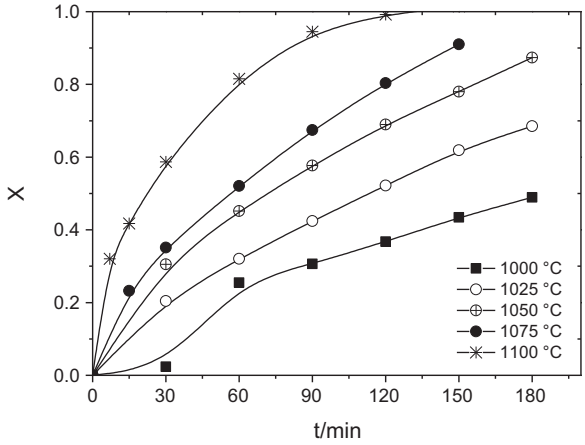

Fig. 3. Chlorination of β-spodumene at different temperatures.

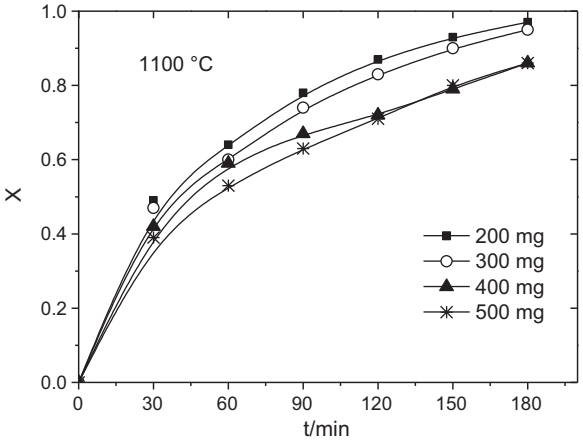

Fig. 4. Effect of the mass of the sample on chlorination of β-spodumene at 1100 °C.

can be seen from this figure that reactivity of the system is slightly affected by the mass of the sample. These observations agree with the results obtained from the study of the effect of temperature i.e. temperature is the most important variable affecting the reaction rate.

6.4. Effect of chlorine partial pressure

The study of the effect of chlorine partial pressure over the chlorination reaction rate of β-spodumene was carried out by diluting the Cl_2 with N_2. The assays were performed at atmospheric pressure, keeping the total flow rate constant at 100 ml/min. Cl_2 partial pressures of 0.2, 0.4, 0.6, and 1 atm were investigated at working temperatures of 1050 °C and 1100 °C. Fig. 5 shows an appreciable variation of the system reactivity with Cl_2 partial pressure for both temperatures.

6.5. Characterization of the reaction residues

SEM micrographs of the residues of β-spodumene chlorination are shown in Fig. 6(a)–(c). Fig. 6(a) shows a micrograph of a particle corresponding to a sample chlorinated at 1100 °C for a period of 60 min from which it can be seen small holes. Fig. 6(b) and (c) show a residue chlorinated for 180 min at 1100 °C which yielded complete conversion. It can be noted from this figure that the original small holes have grown to a great extent.

The EPMA analysis conducted on chlorination residues shows only the presence of the elements O, Al and Si in the proportions shown in Table 2. These results suggest that there is no accumulation of chlorides (LiCl, $CaCl_2$, $MgCl_2$, etc.).

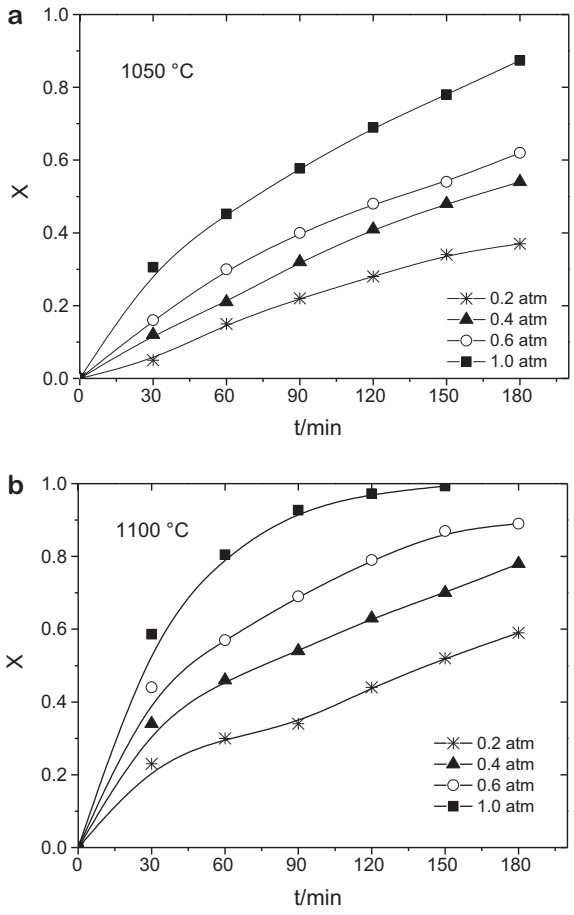

Fig. 5. Effect of Cl_2 partial pressure on the chlorination of β-spodumene: (a) 1050 °C; (b) 1100 °C.

6.6. Kinetic model and mechanism of the reaction

The kinetic model was estimated running the software MODELADO [22] using the experimental data obtained at different temperatures (Fig. 3). The operation conditions used for each assay, shown in Table 3, were entered as a set of inputs to start the estimation.

Where T is the reaction temperature; M_0 initial mass of the sample; d_p diameter of the particle or the least of its characteristic lengths; p_{A0} Cl_2 partial pressure; p_T total pressure; u_s gas velocity.

The model sequential nucleation and growth best fitted the experimental data of β-spodumene chlorination, at different temperatures. The mathematical expression of this model is as following:

$$X = b_1[\ln(1 + b_2 t) - b_2 t/(1 + b_2 t)] \quad (9)$$

Table 2
EPMA analysis, in atomic %, corresponding to chlorination residues obtained at different temperatures and reaction times.

Temperature (°C)	Time (min)	O	Mg	Al	Si	Cl	Ca	Fe
1000	30	50.23	–	14.27	35.40	–	–	–
	90	49.87	–	14.44	35.69	–	–	–
1025	45	43.21	–	16.13	40.66	–	–	–
	75	53.03	–	13.47	33.51	–	–	–
1050	30	52.85	–	14.37	32.79	–	–	–
	90	50.85	–	14.22	34.93	–	–	–
1075	30	53.07	–	14.26	32.67	–	–	–
	75	52.34	–	13.08	34.58	–	–	–
1100	15	51.31	–	14.34	34.35	–	–	–
	45	49.83	–	14.52	35.65	–	–	–

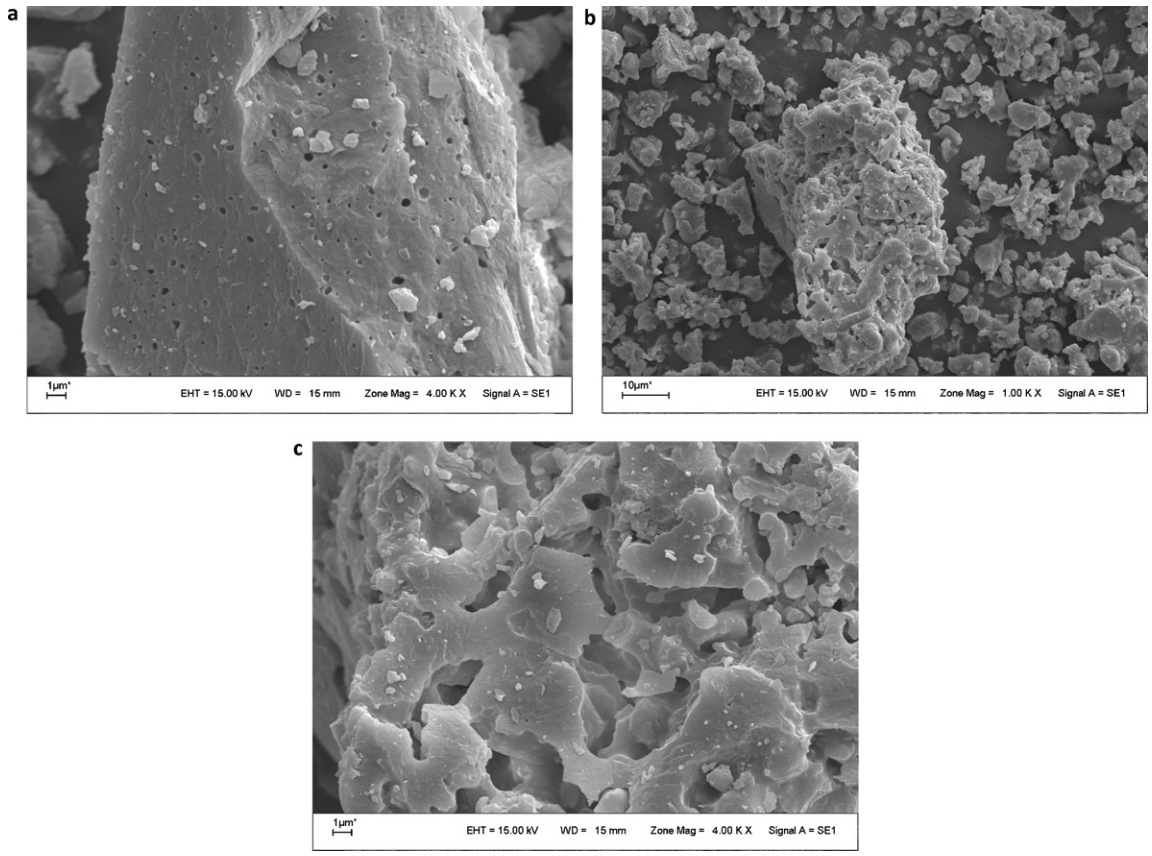

Fig. 6. SEM analysis of the chlorination residue at 1100 °C: (a) surface of particle chlorinated for 60 min; (b) particle chlorinated for 180 min; (c) surface of the particle chlorinated for 180 min.

b_1 and b_2 defined as:

$$b_1 = \sigma_g \Omega^0 N_{E0} \tag{10}$$

$$b_2 = \rho d_p k_{N2} N_{E0} / b M_b r_s \tag{11}$$

where X is the conversion; t the reaction time; σ_g the shape coefficient of nuclei; N_{E0} number of nuclei per unit area; Ω^0 the initial external surface of the particle; b and M_b the stoichiometric coefficient and the molecular weight of the solid reactant, respectively; r_s the heterogeneous reaction rate; ρ density of the reactive solid; k_{N2} kinetic constant of nuclei formation of order 2. The values of the kinetic parameters estimated by the software are shown in Table 4.

Table 3
Experimental conditions of β-spodumene chlorination assays at different temperatures.

T (°C)	1000; 1025; 1050; 1075; 1100
M_0 (mg)	400
d_p (mm)	0.015
p_{A0} (atm)	1
p_T (atm)	1
u_s (cm/s)	0.829

Table 4
Kinetic parameters of the estimated model.

T (°C)	b_1	b_2	$k = b_1 b_2$
1000	0.4357	0.0357	0.0156
1025	0.4301	0.0614	0.0264
1050	0.4134	0.1062	0.0439
1075	0.3667	0.1698	0.0623
1100	0.2699	0.8339	0.2251

The kinetic constant k is defined as the product between b_1 and b_2 [23].

This model is valid for a nucleation order n equal to 2 and a growth factor p equal to 1, indicating that the preferential direction of the germ growth nuclei is in one dimension. The value of n determines the expression of the nucleation reaction rate and p is introduced to take into account the preferential direction of the germ growth in the calculus of the nuclei volume [23]. The results of experimental data adjustment of the chlorination of β-spodumene with the model are shown in Fig. 7. It can be noted that the experimental results and the values predicted by the kinetic model are in

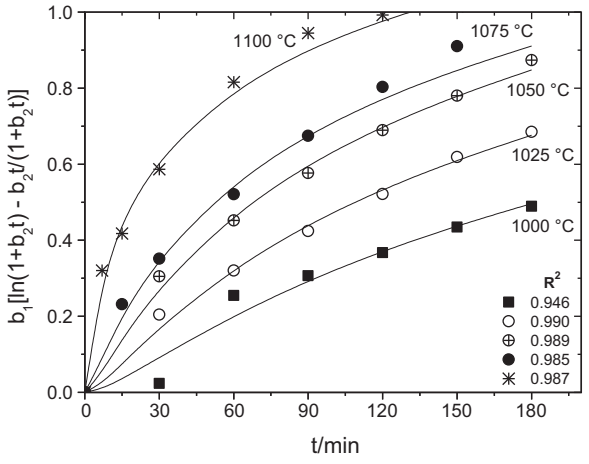

Fig. 7. Mathematical fit of the experimental data of β-spodumene chlorination at different temperatures. (Line) kinetic model; (symbol) experimental data.

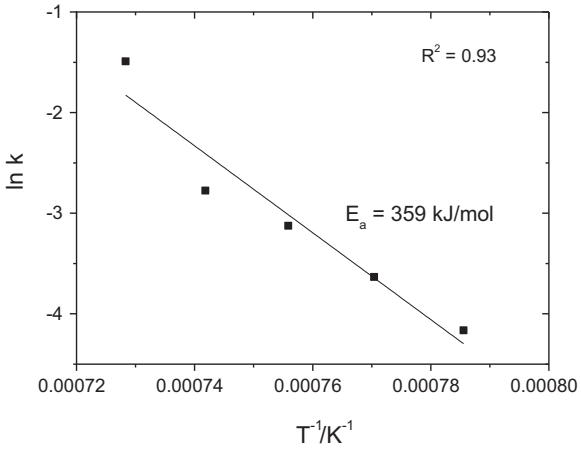

Fig. 8. Arrhenius plot for the chlorination of β-spodumene.

excellent agreement, as can be seen from the values of the squared correlation coefficient, R^2.

The causes of the origin of preferential sites of interaction can be diverse, such as heterogeneities which often have solid surfaces, caused by crystal defects or impurities in the solid [23]. The reaction develops from these preferential points susceptible to chemical interaction, from which the reaction starts and progresses, a fact manifested by the formation of holes that grow from the surface towards the interior of the particle. This growth could be observed in the SEM micrographs (Fig. 6), what may constitute experimental evidence that support the model found for the chlorination of β-spodumene.

Further, taking into consideration the crystal structure of β-spodumene, the defects contained in the structure may account for the preferential sites. The structure of β-spodumene is dominated by interlocking 5-membered rings of (Si, Al) tetrahedra. The five binding oxygens within each ring are almost coplanar and form a fairly regular pentagon. The two oxygens which are closest to the Li form the minimum O—O—O angle of 91° in the oxygen pentagon. The minimum angle of 91° deviates appreciably from ideal pentagon angle of 108°. This may indicate the existence of some strain in the 5-membered rings. Moreover, all the five-membered rings run approximately parallel to either (0 1 0) or (1 0 0) and thus help to create zeolite-like channels. An additional cause for the origin of preferential sites may be the fact that each Li is stuffed in interstitial positions located between two 5-membered rings of (Si, Al) tetrahedra [24].

The activation energy was calculated from a plot of ln k vs. $1/T$ and these results are presented in Fig. 8. The estimated activation energy value of 359 kJ/mol suggests that the chlorination rate is controlled by the superficial chemical reaction between the Cl_2 and the β-spodumene.

The apparent order of reaction with regards to the partial pressure of chlorine was estimated from a graphic of ln k vs. ln p_{Cl2} (Fig. 9), which was built by applying the kinetic model provided by Eq. (9) to the curves in Fig. 5.

Fig. 9a shows that, the reaction order is 0.83 for the temperature of 1050 °C and 1.24 for 1100 °C. The difference between these values may be due to the different processes that take place during the chlorination of β-spodumene. First, the crystalline structure of β-spodumene turns to an aluminum silicate crystalline phase characterized for a lesser content of lithium. As the reaction progresses, two additional crystalline phases (mullite and cristobalite) are formed, constituting also the solid reactant. In addition, as the temperature increases, the chlorination of Al may also occur. This process is characterized by the crystallization of the α-Al_2O_3 phase after the formation of $AlCl_3$ in presence of O_2, as demonstrated by Lopasso et al. [25].

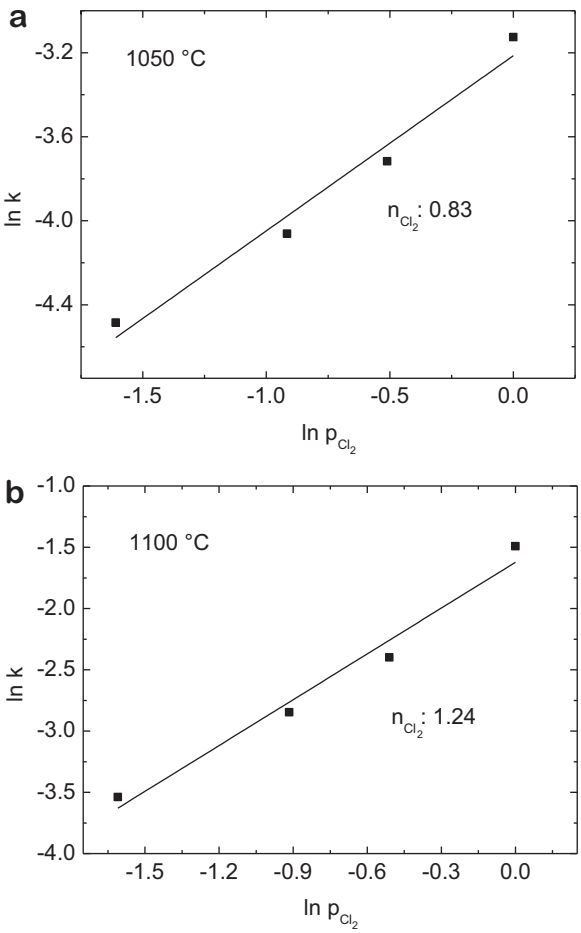

Fig. 9. Estimation of the reaction order between 0.2 and 1 atm.

7. Conclusions

The extraction of lithium through chlorination of β-spodumene with pure Cl_2 is highly dependent on the temperature being significant for temperatures above 1000 °C.

The partial pressure of chlorine has an appreciable effect on the system reactivity, taking into account the values of 0.83 and 1.24 of the apparent reaction order for 1050 and 1100 °C, respectively. Flow rate has a lesser effect on it, but a slight decrease on the conversion of Li_2O at high flow rates suggests that the chlorination of β-spodumene is carried out in the presence of active chlorinating species.

The value found for the apparent activation energy, 359 ± 10 (kJ/mol), indicates that the chemical stage plays a very important role on the control of the reaction rate.

Experimental data fitted the sequential nucleation and growth model with a nucleation of second order and a one-dimensional preferential nucleation.

Acknowledgements

The authors of this work would like to acknowledge FONCyT, CONICET, UNSL, and UNCUYO for the financial support.

References

[1] A. Ebensperger, P. Maxwell, C. Moscoso, The lithium industry: its recent evolution and future prospects, Resour. Policy 30 (2005) 218–231.

[2] I. Ilic, S. Stopic, K. Cerovic, Z. Kamberovic, Study of chlorination of nickel silicate by gaseous chlorine and calcium chloride in the presence of active additives, Scand. J. Metall. 29 (2000) 9–16.
[3] A. Landsberg, Chlorination kinetics of aluminum bearing minerals, Metall. Trans. B 6 (2) (1975) 207–214.
[4] N. Kanari, E. Allain, R. Joussement, J. Mochon, I. Ruiz-Bustaniza, I. Gaballah, An overview study of chlorination reactions applied to the primary extraction and recycling of metals and to the synthesis of new reagents, Thermochim. Acta 495 (2009) 42–50.
[5] R. Orosco, M. Ruiz, L. Barbosa, J. González, Purification of talcs by chlorination and leaching, Int. J. Miner. Process. 101 (2011) 116–120.
[6] C. Davidson, Extraction of metals from mixtures of oxides or silicates, Application No. 116695, Publication No. 4307066, 22/12/1981. International Classifications: C01D 15/04; C01 F 11/28.
[7] C. Davidson, Recovery of lithium from low-grades ores, Application No. 116697, Publication No. US4285914, 25/08/1982. International Classifications: C01D 3/08.
[8] E.D. Wendell Jr., Cyclical vacuum chlorinating processes, including lithium extraction, Application No. PCT/US2005/010273, Publication No. WO 2005/094289 A2, Publication No. WO 2005/094289 A2, 13/10/2005.
[9] L. Barbosa, G. Valente, J. González, Estudio de la extracción de litio de espodumeno mediante cloración y carbocloración, 11° Congreso binacional de metalurgia y materiales, SAM/CONAMET, Rosario, Argentina, 2011.
[10] HSC Chemistry for Windows Software V. 5.1, Outokumpu Research, Pori, Finland, 2003.
[11] D. Hildenbrand, W. Hall, F. Ju, N. Potter, Vapor pressure and vapor thermodynamic properties of some lithium and magnesium halides, J. Chem. Phys. 40 (1964) 2882–2890.
[12] J. Szekely, J. Evans, H. Sohn, Gas-Solid Reactions, Academic Press, New York, 1976.
[13] A. Bidaye, S. Venkatachalam, C. Gupta, Studies on the chlorination of zircon: part I. Static bed investigations, Metall. Mater. Trans. B 30B (1999) 205–213.
[14] M.W. Ojeda, M. del, C. Ruiz, M.E. Godoy, J.B. Rivarola, Recovery of palladium from exhausted catalyst by chlorination: effect of carbon, Trans. Instn. Min. Metall. (Sect. C: Mineral Process. Extr. Metall.) 108 (1999) 33–38.
[15] M. del C. Ruiz, Estudio cinético de la reacción entre trióxido de molibdeno puro y tetracloruro de carbono en fase vapor, Tesis Doctoral, Universidad Nacional de San Luis, Argentina, 1988.
[16] M. del, C. Ruiz, J.B. Rivarola, O.D. Quiroga, Kinetic study of the reaction between molybdenum trioxide and gaseous carbon tetrachloride, Can. J. Chem. Eng. 72 (1994) 289–295.
[17] G. Scheimann, O. Immel, H. Rötger, H.J. Schmidt, Zur thermischen Zersetzung von Tetrachlorkohlenstoffdampfen und ihre reaktionstechnische Auswertung, Z. Phys. Chem. (Neue Folge) 32 (1962) 137–153.
[18] J.M. Smith, Ingeniería de la Cinética Química, segunda edición, Compañía Editorial Continental S. A., México, 1977.
[19] D.W. Sparling, J.R. Glastonbury, Australian JMM Conf. (1973) 455–463.
[20] I. Gaballah, E. Allain, M. Djona, Chlorination kinetics of refractory metals oxides (MoO_3, Nb_2O_5, Ta_2O_5 and V_2O_5), M. Light Metals (1994) 1153–1161.
[21] I. Barin, W. Schuler, On the kinetics of the chlorination of titanium dioxide in the presence of solid carbon, Metall. Trans. B 11 (1980) 199–207.
[22] O.D. Quiroga, Modelado, Software para el tratamiento cinético de transformaciones fluido sólido-reactivo, INIQUI (UNSa – CONICET), SALTA, 2000.
[23] O.D. Quiroga, J.R. Avanza, A.J. Fusco, Modelado cinético de las transformaciones fluido-solido reactivo, Ed. FACENA, Corrientes, 1994.
[24] L. Chi-Tang, R.P. Donald, The crystal structure of $LiAlSi_2O_6$-II ("β-spodumene"), Zeitschrift für Kristallographie 126 (1968) 46–65.
[25] E.M. Lopasso, J.J. Andrade Gamboa, J.M. Astigueta, D.M. Pasquevich, Enhancing effect of Cl2 atmosphere on transition aluminas transformation, J. Mater. Sci. 32 (1997) 3299–3304.